Int j simul model 21 (2022) 4, 603-614
Original scientific paper

# SHAPE CHANGE SIMULATION ANALYSIS OF WHEEL STEEL IN A FOUR-HIGH HOT ROLLING MILL

Liu, G. F.[*]; Cui, X. Y.[*]; Li, Z. Z.[*]; Wang, J. H.[*]; Zhang, X. D.[*] & Bai, Z. H.[*,**,#]

[*] National Cold Rolling Strip Equipment and Process Engineering Technology Research Center of Yanshan University, Qinhuangdao, 066004, China

[**] State Key Laboratory of Metastable Materials Science and Technology, Yanshan University, Qinhuangdao, 066004, China

E-Mail: bai_zhenhua@aliyun.com ([#] Corresponding author)

**Abstract**

To reveal the shape change characteristics during the rolling process of the four-high hot continuous rolling mill, a three-dimensional finite element model was built with the wheel steel 380CL as the sample. The equivalent stress field, strain field, and displacement change of thickness of the wheel steel in each rolling process were analysed, and the field measurement and verification analysis were carried out. Results show that the equivalent stress, strain and thickness displacement of the strip edge gradually increases with the rolling, respectively. Reasonable tension before and after loading can effectively reduce the equivalent stress in the deformation zone and the rolling pressure required during rolling. The difference between the simulated rolling outlet thickness of 7.61 mm and the field measured thickness of 7.69 mm is small, which verifies that the calculation accuracy of the finite element is high. The conclusions obtained in this study provide a basis and reference for the development of similar wheel steel rolling calculation model.

(Received in July 2022, accepted in October 2022. This paper was with the authors 1 month for 2 revisions.)

**Key Words:** Hot Rolling, Continuous Rolling, Plate Shape, Finite Element

## 1. INTRODUCTION

With the transition of Chinese manufacturing industry to high-end, the users have increasingly high requirements for the quality of hot rolled plates and strips. For the evaluation standard of strip quality, it is particularly important whether the shape is good or not. The shape of hot rolled plates directly affects the smooth processing of subsequent products [1, 2]. The hot rolling deformation is a complex metal deformation process, it is easy to have defects such as thickness deviation, uneven mechanical properties and poor shape in the production process. Therefore, many scholars have studied and improved the process means and control methods of hot rolling process [3, 4]. However, there are some limitations in the research of hot rolling process, which cannot be well promoted and applied.

Hot rolled plates and strips are produced under the influence of deformed elastomers-rolls. The elastic deformation of rolls directly affects the sectional shape of the final products. Therefore, the higher requirements are put forward for the calculation accuracy of elastic deformation of rolling mill rolls. At the same time, the hot strip rolling process is a highly nonlinear thermo-mechanical coupling problem. On the one hand, the plastic deformation of rolled piece is affected by the material flow stress, which is directly related to the rolling temperature distribution. On the other hand, the heat of plastic deformation and friction in turn affect the temperature distribution of the rolled piece. Among them, the elastic-plastic finite element method can more truly reflect various states in rolling. When elastic-plastic finite element method is used to analyse metal forming problems, it can not only get the evolution process of plastic zone, the distribution characteristics of stress and strain of plastic deformation body and the change of geometric shape according to the deformation path, but also effectively deal with unloading problems [5-8].

The purpose of this study is to analyse the change rule of the strip shape of each stand during the rolling process of the hot rolling mill. The deformation process of the strip is studied by using the finite element simulation method. The stress and the displacement distribution in the deformation zone during the rolling process are obtained.

## 2. STATE OF THE ART

Current research on the hot rolling process mainly includes the stress and strain distribution of the strip steel in the rolling deformation zone, the optimization and improvement of the rolling process parameters, and the simulation calculation of the thickness of the finished strip steel. Therefore, the three aspects can provide a reference for the research on the change rules of the strip shape of each stand in the rolling process.

Some scholars have studied the stress and strain of strip steel deformation during hot rolling. Wei et al. [9] analysed the coupling mechanism of residual stress, thermal stress and contact stress of work roll in the pinch zone using the transient thermo-mechanical model. Su et al. [10] analysed the influences of deformation temperature and deformation rate on the flow stress of the alloy during hot deformation, and they established the constitutive equation and hot working diagram of the alloy. Kaliyev et al. [11] used MSC SUPER FORGE to develop the three-dimensional geometry and simulation model of the rolling process, and obtained the equivalent stress distribution and temperature field distribution of the strip steel under a single stand. Zhao et al. [12] proposed a tolerance coefficient to describe the attenuation and tolerance ability of each support to longitudinal strain difference, which was the basis of the flatness prediction strategy. John et al. [13] developed a rolling force model to calculate the rolling force of each stand, and combined the rolling force calculated by the model with the roll wear model to better predict the strip shape. Milenin et al. [14] established the elastic-plastic deformation model of hot rolled strip during laminar cooling and the deformation model in the strip coil.

Many scholars have studied the optimization of process parameters in the hot rolling process. Wang and Yan [15] proposed a dynamic model of the hot strip rolling mill vibration resulting from entry thickness deviation and studied the dynamic characteristics of this model. Kim et al. [16] proposed a model to predict the distribution of rolling force and tension of hot rolled strip by considering the influence of pre deformation near the roll entrance before the strip enters the bite zone. Suguhiro et al. [17] developed a new method of high-precision online shape prediction model based on matrix model by taking rolling force and tension into account through experiments and finite element analysis. Garber et al. [18] developed the calculation program of the main drive power of the hot rolling wide strip mill, which reduced the contact stress of the roll by redistributing the tension reduction and tension between the stands and increasing the temperature of semi-finished products. Li et al. [19] proposed a shape preset strategy to allocate the crown of the finishing mill according to the size of the shape control domain of each stand. Jung and Im [20] developed a fuzzy control algorithm to study the influence of front and rear tension on reducing the thickness deviation of hot rolled strip.

Other scholars used the finite element method to simulate the hot rolling results. Xie et al. [21] established the material constitutive model through the experimental results of Gleeble 3800 thermal simulator at different temperatures and strain rates, thus obtaining a new three-dimensional finite element simulation method for the shape and flatness of high-strength steel strip. Schindler et al. [22] simulated the operation problems in the hot rolling process of wide and thick products and verify the correctness of the shape model. Pesin and Pustovoytov [23] found that the mechanism of crack movement during plate rolling was the slab front and rear surface tilt caused by the temperature gradient of upper and lower surfaces. Chai et al. [24]

used the flatness calculation model to analyse and compare the flatness and longitudinal residual stress evolution during the rolling process of thick plate and thin plate. Aridi et al. [25] drew the temperature field after the last pass through mathematical modelling and on-site temperature measurement, and they found the cooling curve under various operating conditions. Overhagen and Mauk [26] calculated the crown of the thermal work roll by using the axisymmetric numerical solution of the thermal equation of the work roll, and they obtained the evolution process of the strip steel profile.

In this study, based on the plate deformation in the hot rolling process, the finite element mesh was refined and divided according to the actual assembly and structure of the rolls by indenting the rolls of each stand, and the calculation process was simplified. The quarter rolling of typical products, the deformation zones in each pass of the hot rolling process and the whole hot rolling process were completed. The strip displacement distribution of each pass deformation zone was analysed, and the change rule of strip shape and the thickness distribution of finished strip during the rolling process of the four-high hot rolling mill were obtained.

# 3. METHODOLOGY

## 3.1 Geometric modelling and mesh unit

To get the deformation characteristics of the rolling system, the model of the rolling system was simplified. The rolled piece during the simplified model was regarded as the rectangular piece. Considering for the deformation symmetry, a quarter of the model was taken as the object, the lateral for symmetry plane was at the centre of the plate width 1/2, thick for the symmetry plane was at the centre of the thickness and upper half. The two-dimensional model was built in CAD software, then imported in the Marc Mentat software to carry on the grid division, as shown in Fig. 1 a.

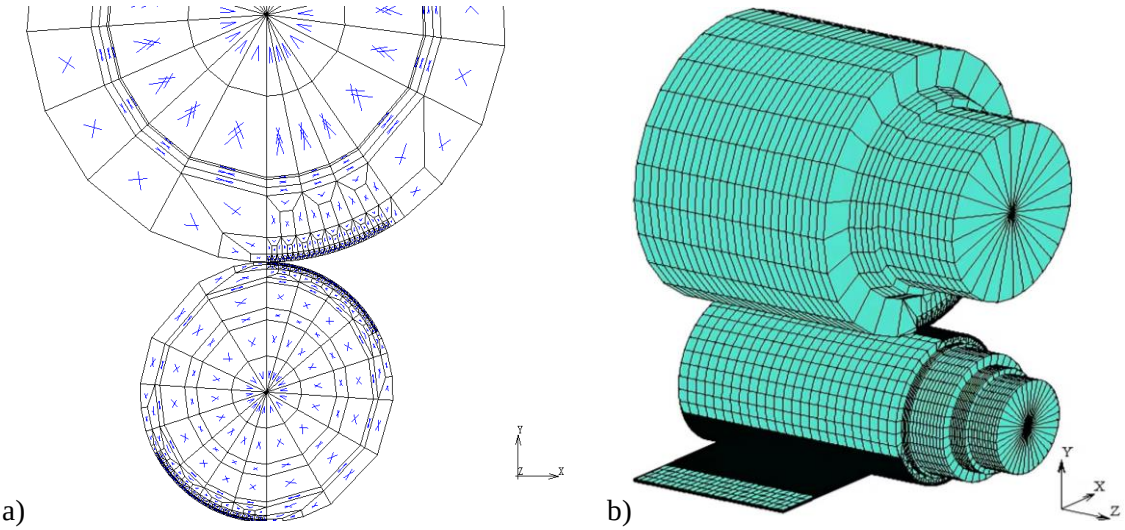


Figure 1: Support roll and work roll; a) plan of support roll and work roll, b) three-dimensional model.

Since the quadrilateral meshes are better than the quality of the triangle grids, the modelling was divided into four node quadrilateral meshes [27-29]. The contact part of the unit was meshed on the elaboration to save computation time and ensure the calculation precision. As shown in Fig. 1 b, in support roll and rolling piece on the circumference of a circle of the contact, the mesh density was increased from the centre to the outer circumference direction gradually. The work roll and strip contact area of the meshes was shown in Fig. 2.

Both the support roll and the work roll were treated as elastomers. In order to make the support roll and the work roll rotate around their respective axes respectively, the large displacement option should be enabled in the analysis option. The elastomer and the rigid body were pasted together through contact, and the rotation of the rigid body drived the rotation of the elastomer roll. In this model, the driving roller was the work roller. The work roller drived the support roller to rotate through friction, and the friction between the work roller and the rolling piece drived the rolling piece to move through friction.

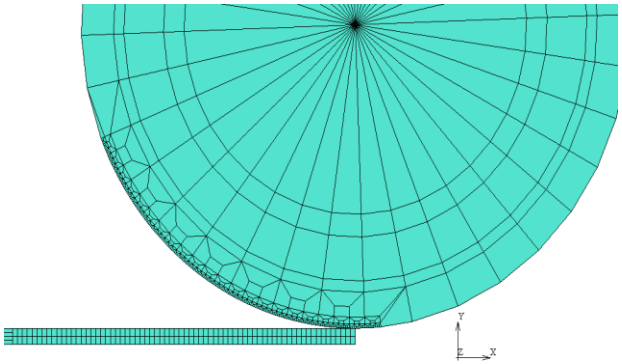

Figure 2: Meshes in contact area.

### 3.2 Type parameter setting

According to 2050 hot rolling unit rolling process parameters, the geometric parameters and material properties of the model are shown in Table I.

Table I: Geometric parameters and material properties of the model.

| **Support roll diameter** (mm) | **Support roll length** (mm) | **Work roll diameter** (mm) | **Work roll length** (mm) | **Elastic modulus** (GPa) | **Poisson's ratio** |
|---|---|---|---|---|---|
| 1440-1600 | 3200 | 700-850 | 3300 | 210 | 0.30 |

### 3.3 Boundary conditions and contact definition

Due to the symmetry of the rolling finite element model, the symmetry plane constraint was established to limit the displacement of the node of the model on the symmetry plane.

The constraints of the support roll in the model were to limit the displacement of the main control point of the support roll in the x and y directions, setting the displacement under pressure of 7.3 mm in the y direction, and fixing the rotation in the y direction. The displacement of the main control point of the work roll in the x direction and the rotation in the y direction were defined, and the rotation radian of the work roll in the z direction was given.

It is difficult to simulate the conveyance and biting process of the plate belt in the calculation, so the calculation was simplified. The simplified method was to put the rolled piece into the roll seam at first, give the back-up roll a pressure displacement, and then drive the work roll to rotate the rolled piece. The calculation results of the steady rolling state were only analysed.

### 3.4 Material model

The rolled piece CW-15 was elastic-plastic material. The material was complied with Von Mises yield criterion and the yield limit was 204.6 MPa.

The deformation process of seven passes was simulated during 380CL rolling of wheel steel. The first three stands are selected to be mainly responsible for large reduction to reduce

the strip crown, and the last four stands are mainly responsible for controlling the shape and roughness.

The process parameters for rolling wheel steel 380CL in 2050 hot rolling mill are shown in Table II. The thickness of incoming material is 43.05 mm, the width is 1615 mm, and the measured final rolling outlet thickness is 7.69 mm. The rolled strip steel shall be 380CL product 2 of the actual steel in production. The model parameters were modified to describe the yield criterion of the large deformation elastoplastic model. The friction condition was the shear friction model based on the equivalent stress.

Table II: Rolling process parameters of the model.

| **Passes** | **Outlet thickness** (mm) | **Rolling force** (kN) | **Work roll bending force** (kN) | **Friction coefficient** | **Tension** (MPa) | **Deformation resistance** (MPa) | **Initial temperature of rolled piece** (℃) |
|---|---|---|---|---|---|---|---|
| 1 | 30.22 | 23137 | 800 | 0.30 | 483 | 171.1 | 980 |
| 2 | 21.84 | 24353 | 800 | 0.30 | 491 | 204.6 | 959 |
| 3 | 15.66 | 21817 | 800 | 0.30 | 501 | 206.8 | 941 |
| 4 | 12.31 | 19376 | 800 | 0.30 | 552 | 243.3 | 928 |
| 5 | 10.30 | 15733 | 650 | 0.30 | 610 | 320.8 | 903 |
| 6 | 8.71 | 13308 | 650 | 0.30 | 699 | 270.5 | 880 |
| 7 | 7.69 | 12903 | 650 | 0.30 | 749 | 311.3 | 864 |

# 4. RESULTS AND DISCUSSION

## 4.1 Analysis of 1/4 rolling process

The load was applied to the model established in Fig. 3. The support roll was pressed down by 7.3 mm, and a positive bending roll force of 800 kN was applied to the centre node of the work roll. The tensile stress before and after the rolled piece was 491 MPa, the inlet thickness of the rolled piece was 30.22 mm, the plate width was 1550 mm, and the friction coefficient between the rolled piece and the rolled piece was set as 0.3. Fig. 3 shows the nephogram of the equivalent stress distribution under roll pressure and rolling steady-state in the rolling simulation process.

As can be seen from Fig. 3, the maximum stress occurs at the diameter of the support roll and the work roll, and the maximum value is 1268 MPa, the maximum equivalent stress of the rolled piece is about 242.2 MPa, and the average equivalent stress in the deformation zone of the rolled piece is about 160 MPa. Since the 1/4 model established is symmetric in the y and z directions, the calculated thickness should be multiplied by 2. The steady-state thickness of the rolled piece is 21.40 mm, which is 0.44 mm different from the actual thickness measurement of 21.84 mm, meeting the accuracy requirements. Therefore, the finite element model can simulate the hot rolling process realistically.

## 4.2 Equivalent stress distribution in each pass deformation zone

According to the rolling process parameters in Table II, the parameters of each pass, such as the amount of pressure, the bending force of the work roll, the material and deformation resistance of the strip, the initial temperature of the rolling piece and the tension before and after were set in the Marc software, and the corresponding initial conditions and boundary conditions were also set. After setting the parameters of each working condition, the task was submitted for solving calculation. Fig. 4 shows the nephogram of the equivalent stress distribution in the rolling deformation area.

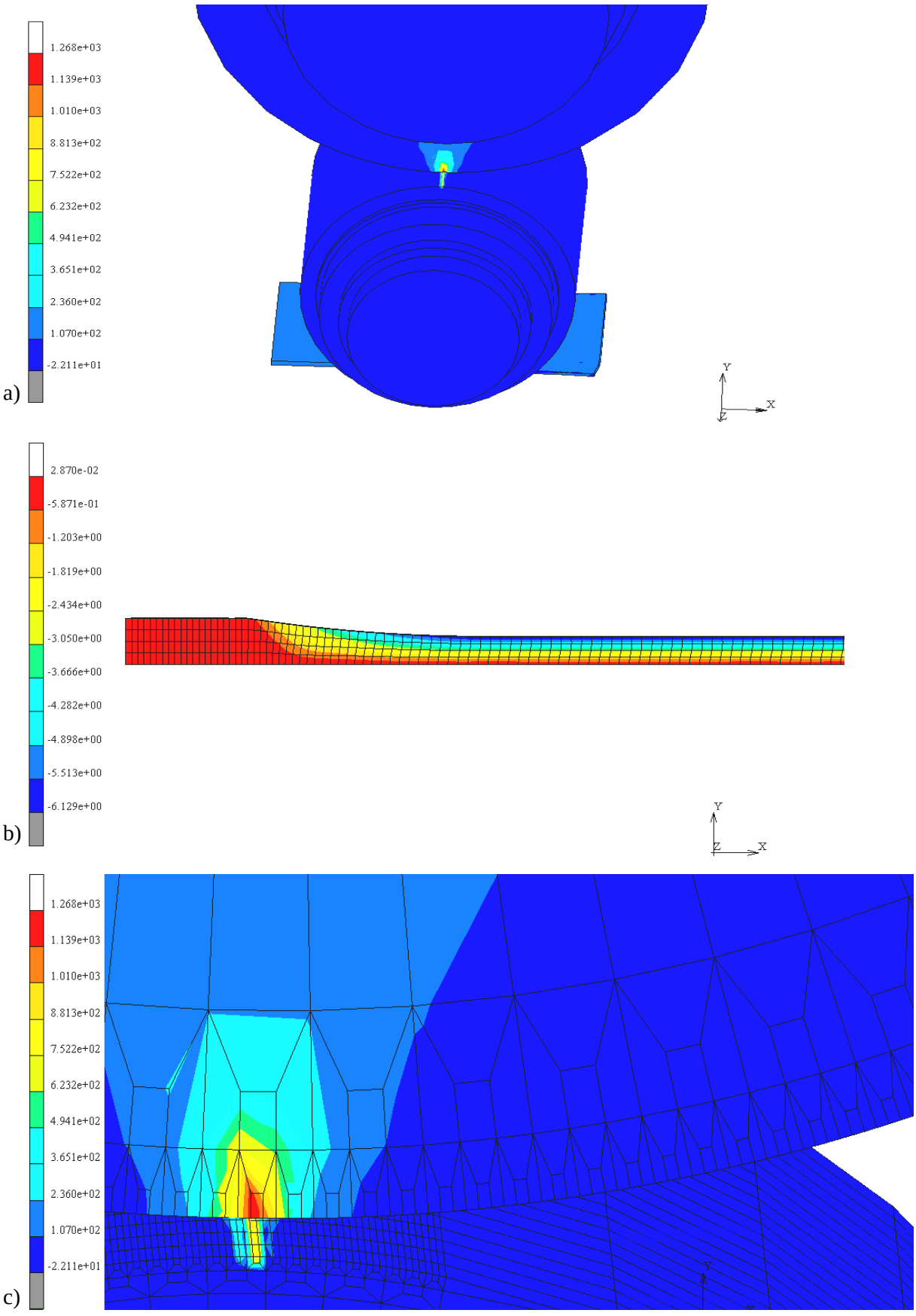


Figure 3: Distribution results of equivalent force; a) press down to 7.3 mm, b) thickness distribution of rolled piece in y direction, c) overall stress distribution in rolling steady state.

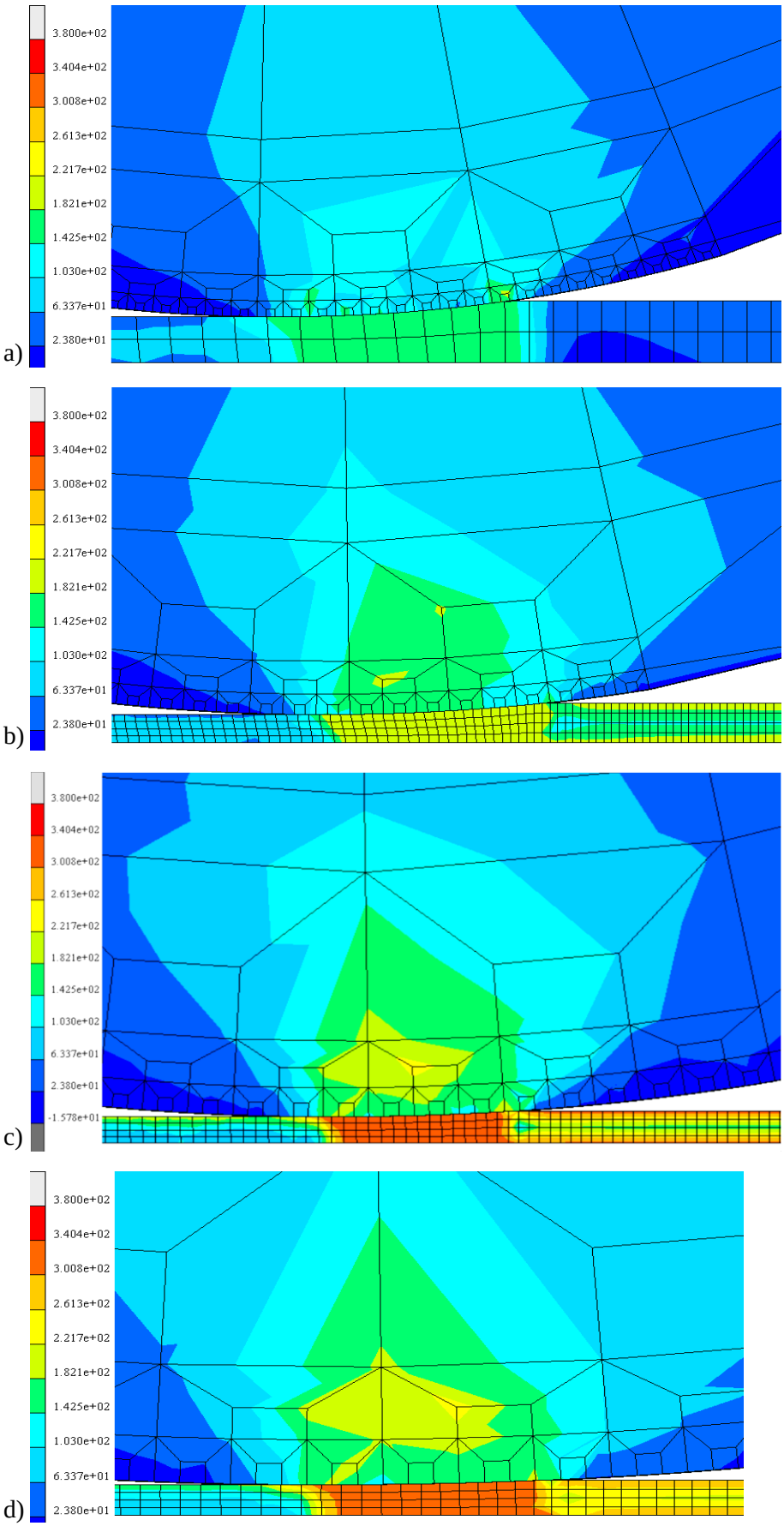


Figure 4: Cloud chart of equivalent stress distribution; a) first pass, b) third pass, c) fifth pass, d) seventh pass.

As can be seen from Fig. 4, the equivalent stress increases gradually. The stress in the deformation zone of the rolled parts in the first pass is about 170 MPa, and the stress in the seventh frame increases to about 300 MPa. The thinner the strip thickness is, the greater the deformation resistance is. The equivalent stress in the deformation zone can be effectively reduced by reasonable tension before and after loading the strip, thus reducing the required rolling pressure.

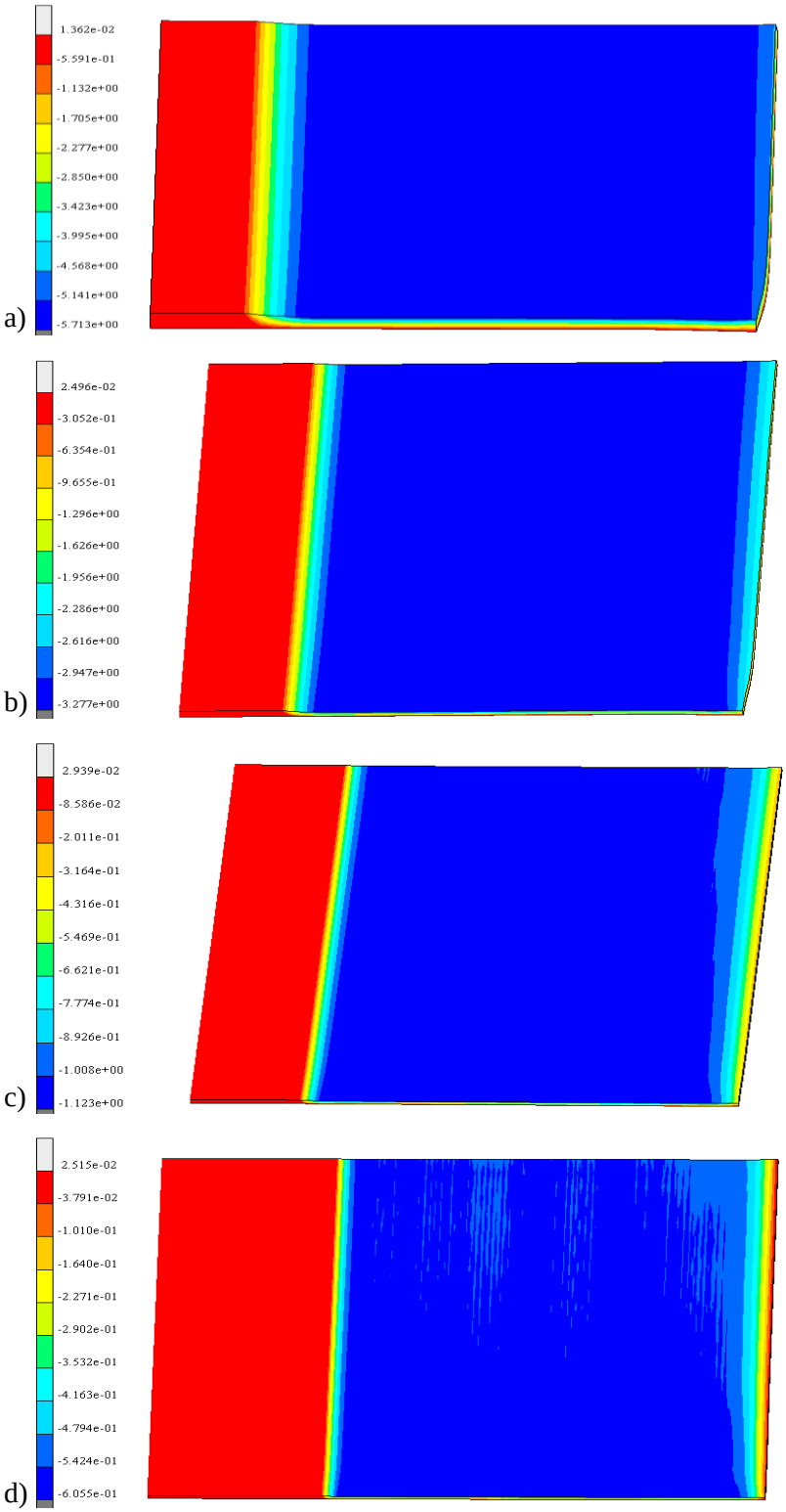


Figure 5: Variation distribution of thickness displacement in the deformation zone; a) first pass, b) third pass, c) fifth pass, d) seventh pass.

### 4.3 Strip steel displacement distribution in each pass deformation zone

After the finite element solution being completed, the distribution cloud diagram of the strip displacement change in each pass deformation area was obtained, as shown in Fig. 5. The rolled element was selected to extract the data of the width direction of each pass plate and the data was imported into the excel sheet for the drawing of outlet thickness.

In the simulation of strip rolling process, it is found that the elastic deformation exists at both the inlet and outlet of strip. As we all know, the elastic recovery of strip steel at the exit cannot be ignored. It is just like the plastic deformation caused by metal loading, and then the metal is unloaded to return to the state of stress zero according to the opposite direction of the original elastic deformation. The loading and unloading process produces the elastic recovery. The strip gets the maximum deformation at the very bottom of the work roll. The appearance of recovery phenomenon makes the strip cannot maintain the shape in the roll gap after rolling out, which makes the actual shape of the strip different from the shape in the roll gap, that is, the thickness value of the strip after rolling out of the roll should be the value of the load roll gap of the work roll plus the elastic recovery of the strip.

As can be seen from Fig. 6, the thickness of each pass outlet in the direction of plate width of the strip changes little in the centre area, and the edge thickness of the strip decreases slightly compared with the centre area. According to the calculation, from the first pass to the seventh pass, the plate convexity decreases successively. The first pass convexity is the largest, which is 0.25 mm, and the seventh pass convexity is the smallest, which is 0.11 mm. The outlet thickness of each pass calculated by simulation is in good agreement with the measured outlet thickness. The outlet thickness of the seventh pass calculated by finite element method is 7.61 mm, and the measured value is 7.69 mm.

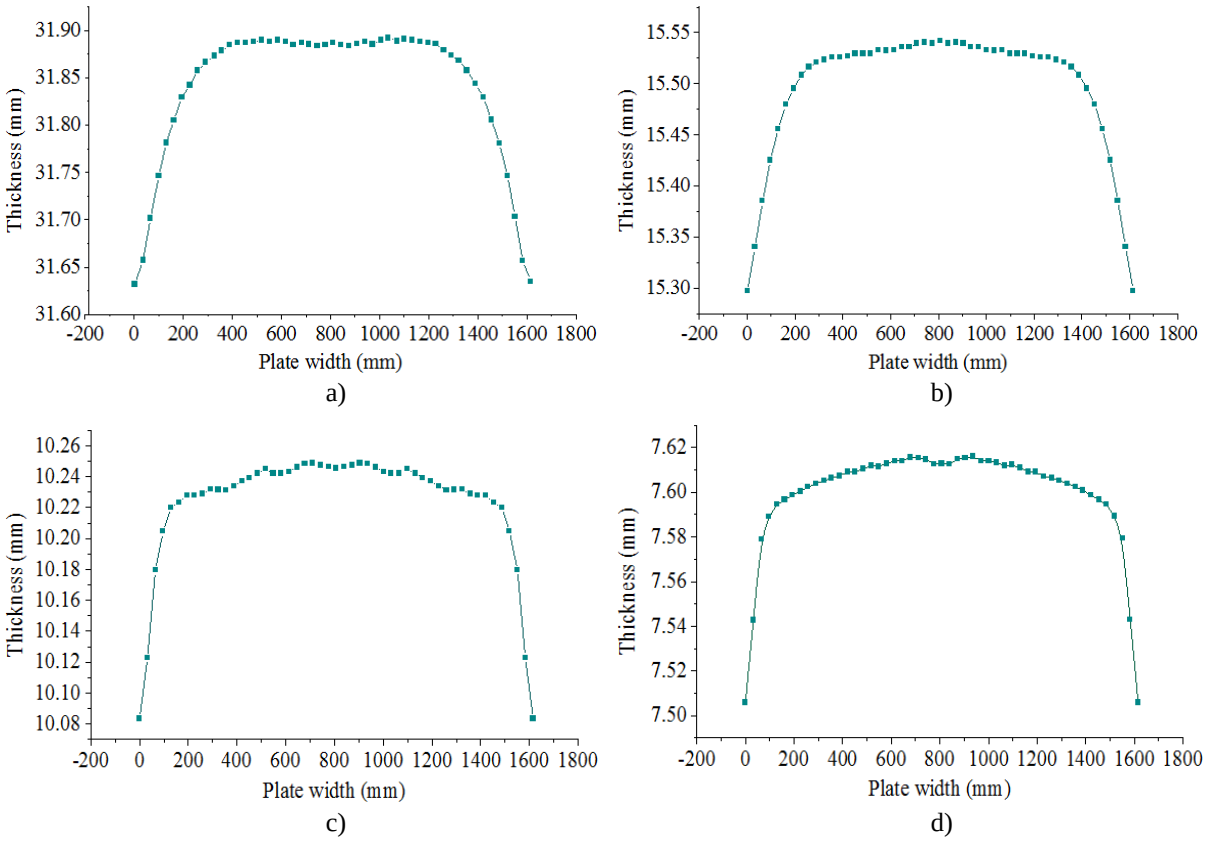


Figure 6: The outlet thickness in rolling deformation zone; a) first pass, b) third pass, c) fifth pass, d) seventh pass.

## 5. CONCLUSIONS

The rolling process of four-high hot rolling mill was simulated by establishing a 1/4 finite element model, and the equivalent stress distribution, the displacement change of each pass deformation zone in the rolling process were analysed. The main conclusions were obtained as followings:

(1) The four-high roll rolling model was used to simulate the rolling of 380CL wheel steel produced on site for seven passes. The equivalent stress field, strain field, thickness change and exit thickness curve of each pass of strip steel deformation zone were obtained.

(2) In the rolling process, the stress, strain and thickness displacement of the strip edge gradually increase. Reasonable tension before and after loading can effectively reduce the equivalent stress in the deformation zone, thus reducing the rolling pressure required.

(3) The difference between the exit thickness of 7.61 mm from the simulation results and the field measured of 7.69 mm is small, which verifies the calculation accuracy of the model and provides the reference for the subsequent model development.

This study provides a reference for the calculation and simulation of the transverse distribution of the thickness of the plate and strip in the hot rolling unit. However, the actual rolling process of hot rolling is very complex, so the thickness and shape of the plate and strip will be simulated through more detailed conditions in combination with the field tests.

## ACKNOWLEDGEMENT

This work was supported by the Funding Project of Central Guiding for Local Science and Technology Development (206Z1004G), and the Project of Tangshan Science and Technology Plan (20140209C), China.

## REFERENCES

[1] Muntin, A. V. (2019). Advanced technology of combined thin slab continuous casting and steel strip hot rolling, *Metallurgist*, Vol. 62, No. 9, 900-910, doi:10.1007/s11015-019-00747-5

[2] Szelinga, D.; Czyzewska, N.; Klimczak, K.; Kusiak, J.; Kuiziak, R.; Morkisz, P.; Oprocha, P.; Pietrzyk, M.; Poloczek, L.; Przybylowicz, P. (2022). Stochastic model describing evolution of microstructural parameters during hot rolling of steel plates and strips, *Archives of Civil and Mechanical Engineering*, Vol. 22, No. 3, Paper 139, 10 pages, doi:10.1007/s43452-022-00460-2

[3] Ma, X. B.; Wang, D. C.; Liu, H. M.; Wen, C. C.; Zhou, Y. (2018). Large concave roll technology for hot rolled silicon steel, *Ironmaking & Steelmaking*, Vol. 45, No. 1, 66-75, doi:10.1080/03019233.2016.1240841

[4] Yu, J. X.; Sun, J.; Zhang, D. H. (2021). Hit prediction of hot strip head thickness based on depth learning, *Steel*, Vol. 56, No. 9, 19-25, doi:10.13228/j.boyuan.issn0449-749x.20210044

[5] Andersson, M.; Finnström, R.; Nylén, T. (2004). Introduction of enhanced indefinite chill and high speed steel rolls in European hot strip mills, *Ironmaking & Steelmaking*, Vol. 31, No. 5, 383-388, doi:10.1179/030192304225018208

[6] Rasovic, N.; Cekic, A.; Kaljun, J. (2022). Design and simulation of the controlled failure of custom-built rigid shaft coupling, *International Journal of Simulation Modelling*, Vol. 21, No. 3, 383-394, doi:10.2507/IJSIMM21-3-596

[7] He, A. R. (2022). Current situation and future development of shape control technology for hot strip rolling, *Steel Rolling*, Vol. 39, No. 3, 1-10, doi:10.13228/j.boyuan.issn1003-9996.20220301

[8] Khan, M. A. A.; Sheikh, A. K. (2021). Simulation-based mould design, life prediction and reliability assessment of a valve body, *International Journal of Simulation Modelling*, Vol. 20, No. 2, 219-230, doi:10.2507/IJSIMM20-2-543

[9] Wei, C.; Song, S. X.; Zhang, Z. X. (2022). Evaluation of elastic-plastic deformation in HSS work roll under coupling of residual stress thermal stress and contact stress during hot rolling,

*Materials Today Communications*, Vol. 33, Paper 104613, 11 pages, doi:10.1016/j.mtcomm.2022.104613

[10] Su, Y. L.; Luo, B. H.; Bai, Z. H.; Mo, W.; He, C. (2021). Hot deformation behavior and hot-rolling process of Al-Mg-Si-In alloy, *Cailiao Daobao / Materials Reports*, Vol. 35, No. 20, 20137-20142, doi:10.11896/cldb.20090118

[11] Kaliyev, Y. B.; Baizhumanov, K. D.; Tursymbekova, Z. Z.; Zhumanov, M. A.; Smailova, G. A.; Azilkiyasheva, M. M.; Zhauyt, A. (2021). Study of stress-strain state billets when rolling in a continuous mill of hot-rolled thin stripes using MSC Super Forge, *Metallurgy*, Vol. 60, No. 1-2, 159-161

[12] Zhao, J. W.; Wang, X. C.; Yang, Q.; Wang, Q.; Liu, C.; Song, G. (2019). High precision shape model and presetting strategy for strip hot rolling, *Journal of Materials Processing Technology*, Vol. 265, 99-111, doi:10.1016/j.jmatprotec.2018.10.005

[13] John, S.; Sikdar, S.; Mukhopadhyay, A.; Pandit, A. (2006). Roll wear prediction model for finishing stands of hot strip mill, *Ironmaking & Steelmaking*, Vol. 33, No. 2, 169-175, doi:10.1179/174328106X80091

[14] Milenin, A.; Kuziak, R.; Lech-Grega, M.; Chochorowski, A.; Witek, S.; Pietrzyk, M. (2016). Numerical modeling and experimental identification of residual stresses in hot-rolled strips, *Archives of Civil and Mechanical Engineering*, Vol. 16, No. 1, 125-134, doi:10.1016/j.acme.2015.08.002

[15] Wang, X. X.; Yan, X. Q. (2019). Dynamic model of the hot strip rolling mill vibration resulting from entry thickness deviation and its dynamic characteristics, *Mathematical Problems in Engineering*, Vol. 2019, Paper 5868740, 11 pages, doi:10.1155/2019/5868740

[16] Kim, Y. K.; Kwak, W. J.; Shin, T. J.; Hwang, S. M. (2010). A new model for the prediction of roll force and tension profiles in flat rolling, *ISIJ International*, Vol. 50, No. 11, 1644-1652, doi:10.2355/isijinternational.50.1644

[17] Fukushima, S.; Washikita, Y.; Sasaki, T.; Nakagawa, S.; Buei, Y.; Yakita, Y.; Yanagimoto, J. (2014). Mixed scheduled rolling of high tensile strength and mild steel using a high-accuracy profile model in hot strip finishing mill, *Tetsu-to-Hagane*, Vol. 100, No. 12, 1499-1507, doi:10.2355/tetsutohagane.100.1499

[18] Garber, E. A.; Kozhevnikova, I. A.; Tarasov, P. A.; Traino, A. I. (2007). Effect of sliding and rolling friction on the energy-force parameters during hot rolling in four-high stands, *Russian Metallurgy (Metally)*, Vol. 2007, No. 6, 484-491, doi:10.1134/S0036029507060080

[19] Li, H. J.; Zhao, X. L.; Xu, J. Z.; Wang, G.; Xiao, Y. (2009). Shape present strategy for hot strip mill, *Journal of Iron and Steel Research*, Vol. 21, No. 10, 17-20, doi:10.13228/j.boyuan.issn1001-0963.2009.10.005

[20] Jung, J.-Y.; Im, Y.-T. (1999). Fuzzy control algorithm for the prediction of tension variations in hot rolling, *Journal of Materials Processing Technology*, Vol. 96, No. 1-3, 163-172, doi:10.1016/S0924-0136(99)00340-4

[21] Xie, H. B.; Li, L. J.; Liu, T. W.; Wang, E. R.; Liu, X.; Jiang, Z. Y. (2019). Three dimensional finite element simulation of strip shape and flatness of high strength steel, *Key Engineering Materials*, Vol. 794, 232-245, doi:10.4028/www.scientific.net/KEM.794.232

[22] Schindler, I.; Hadasik, E.; Kopeček, J.; Kawulok, P.; Fabik, R.; Rusz, S.; Kawulok, R.; Jablonska, M. (2015). Optimization of laboratory hot rolling of brittle Fe-40at.%Al-Zr-B aluminide, *Archives of Metallurgy and Materials*, Vol. 60, No. 3, 1693-1701, doi:10.1515/amm-2015-0293

[23] Pesin, A.; Pustovoytov, D. (2015). Research of edge defect formation in plate rolling by finite element method, *Journal of Materials Processing Technology*, Vol. 220, 96-106, doi:10.1016/j.jmatprotec.2015.01.001

[24] Chai, X. J.; Li, H. B.; Zhang, J.; Zhou, Y.; Ma, H.; Zhang, P. (2018). Flatness analysis and control of strips with different thickness in 2250 mm hot tandem rolling, *Steel Research International*, Vol. 89, No. 12, Paper 1800404, 10 pages, doi:10.1002/srin.201800404

[25] Aridi, M. R.; Noda, N.-A.; Sano, Y.; Takata, K.; Sun, Z.; Takase, Y. (2022). Fatigue failure risk evaluation of bimetallic rolls in four-high hot rolling mills, *Fatigue & Fracture of Engineering Materials & Structures*, Vol. 45, No. 4, 1065-1087, doi:10.1111/ffe.13651

[26] Overhagen, C.; Mauk, P. J. (2018). A model for prediction of profile and flatness of hot and cold rolled flat products in four-high mills, *AIP Conference Proceedings*, Vol. 1960, No. 1, Paper 040015, 6 pages, doi:10.1063/1.5034869

[27] Wang, S.-R.; Liu, Z.-W.; Qu, X.-H.; Fang, J.-B. (2009). Large deformation mechanics mechanism and rigid-gap-flexible-layer supporting technology of soft rock tunnel, *China Journal of Highway and Transport*, Vol. 22, No. 6, 90-95

[28] Luo, T.; Wang, S. R.; Zhang, C. G.; Liu, X. L. (2017). Parameters deterioration rules of surrounding rock for deep tunnel excavation based on unloading effect, *DYNA*, Vol. 92, No. 6, 648-654, doi:10.6036/8554

[29] Wang, S. R.; Xiao, H. G.; Zou, Z. S.; Cao, C.; Wang, Y. H.; Wang, Z. L. (2019). Mechanical performances of transverse rib bar during pull-out test, *International Journal of Applied Mechanics*, Vol. 11, No. 5, Paper 1950048, 15 pages, doi:10.1142/S1758825119500480